



LAWRENCE
LIVERMORE
NATIONAL
LABORATORY

Macroscopic Superlattices of CdSe Colloidal Nanocrystals: Appearance and Optical Properties

N. Zaitseva, L. Manna, F. Leon, D. Gerion, C.
Saw, G. Galli

April 8, 2004

Advanced Materials

Disclaimer

This document was prepared as an account of work sponsored by an agency of the United States Government. Neither the United States Government nor the University of California nor any of their employees, makes any warranty, express or implied, or assumes any legal liability or responsibility for the accuracy, completeness, or usefulness of any information, apparatus, product, or process disclosed, or represents that its use would not infringe privately owned rights. Reference herein to any specific commercial product, process, or service by trade name, trademark, manufacturer, or otherwise, does not necessarily constitute or imply its endorsement, recommendation, or favoring by the United States Government or the University of California. The views and opinions of authors expressed herein do not necessarily state or reflect those of the United States Government or the University of California, and shall not be used for advertising or product endorsement purposes.

Macroscopic superlattices of CdSe colloidal nanocrystals: appearance and optical properties**

By Natalia Zaitseva, Liberato Manna, Francisco Leon, Daniele Gerion, Cheng Saw,
and Giulia Galli*

Two and three dimensional assemblies of colloidal nanocrystals (NCs) have been of great interest during recent years [1-3]. While size-dependent optical and electronic properties of isolated particles are particularly important for fundamental research, studies of their ordered assemblies provide a transition path to the engineering of materials and devices for future practical applications. Assemblies of NCs of different materials, such as semiconductors, metals and metal oxides, have been reported in the literature during recent years [4-7]. However, perfect, crystallographic-ordered assemblies of colloidal NCs or colloidal superlattices (SLs) have been observed so far only using transmission (TEM) and scanning electron microscopy (SEM) in a very small scale of a few hundred nanometers, while macroscopic characterization and device application demonstrations have been performed mainly on amorphous, randomly packed powders of NCs [8, 9]. To make SLs available for traditional methods of characterization, they should be obtained in a sufficiently large size. For colloidal NCs soluble in variety of solvents, simple growth from solution seems to be an appropriate choice to produce SLs. In solution, NCs act as large molecules that, as shown previously [1, 8], can form nano-scale ordered assemblies by the classical Frank-Cabrera mechanism [10] of crystal growth. It is, however, not clear how such ordered structures will look at larger scale. Will they grow as 3-D faceted shapes of extended sizes, or will they form poly-domain structures with local crystallographic arrangement? Taking into account the complex nature of colloidal NCs consisting of relatively big crystalline cores surrounded by large organic surfactant molecules, it is hard to imagine easy formation of large-scale faceted SLs. Spontaneous growth of perfectly faceted crystals requires precisely uniform size, shape and orientation of building units within the crystallographic lattice. This makes the distribution of sizes and shapes that always exist in NCs one more reason to prevent faceting. At the same time, formation of faceted SLs from colloidal solutions has been reported in a number of works [1, 6, 8, 11]. Two recent publications in this journal [12,13] were devoted to the case of CdSe that, for its well-known properties, can be

considered as a model NC material. These publications stated that perfectly shaped hexagonal platelets obtained from a toluene solution of CdSe NCs were faceted SLs. The size of the crystals (up to 200 μm) was large enough to observe them in an optical microscope, but apparently too small for the separation and characterization by macroscopic techniques. Therefore no optical characterization was presented, and the conclusion was made on the basis of TEM images of small fragments that did not show any visible faceting. It is important to say here that, despite the fact that the authors used a special triple-solvent “controlled oversaturation technique”, formation of these hexagonal platelets is not rare in CdSe NC solutions and had been discussed previously in the connection with SL formation [1]. In our experiments with CdSe NCs, we frequently observed them to form spontaneously in relatively large number and size. Such common and easy formation of these crystals stimulated us to take a closer look at their nature. Here we present the results of our investigations, together with new attempts to obtain micron-scale SLs of CdSe NCs suitable for direct characterization by combination of electron microscopy with macroscopic techniques, such as optical polarization microscopy, x-ray diffraction, and photoluminescence spectroscopy.

CdSe NCs were synthesized by commonly used techniques in trioctylphosphine oxide (TOPO) solutions [14-16] that allow for obtaining narrow size and shape distribution. Final powders analyzed by X-ray diffraction, never showed the presence of any crystallites except for CdSe. Dry NCs were dissolved in toluene, although in some cases chloroform solutions were also used. Examination of NCs precipitated after solvent evaporation on a microscope slide or TEM grid never revealed formation of any microscopic faceted shapes in freshly prepared solutions, neither in optical nor in electron microscopes. However, if the initial diluted solutions of NCs were left to evaporate slowly, faceted hexagonal platelets formed in a few weeks. The average size of the crystals was in the range of 20-200 μm , which could be easily observed by optical microscopy in the solid layer left after solvent evaporation. In many cases, their formation could be observed *in-situ* directly in the solution drops. The color, appearance and shapes of the crystals were identical to those presented in [12,13]. To assure that we were dealing exactly with the same type of crystals, in parallel to our runs, we reproduced the “controlled oversaturation” technique [12, 13], in which the NC solution was placed in a narrow glass tube with additional layers of propanol and methanol over it. Similar hexagons, as well as some other rhomboid or elongated shapes obtained by both approaches are presented in Fig. 1a-

d. Careful optical observation and measurements of angles between the edges showed that all these crystals belonged to the same crystallographic form. The main striking feature that probably led to the assumption that they could be faceted SLs is their optical color, that varies from yellow to red and very often exactly coincides with the color of parent CdSe NCs. Fig. 1a shows irregular-shaped agglomerates of NCs (circled) that, in their color, are not distinguishable from the faceted crystal next to them. It is not easy to perform direct structural analysis of these crystals using traditional NC investigation tools. Typical thickness of the crystals, on the order of microns, makes them not transparent for TEM. SEM, Energy Dispersive Spectroscopy (EDS) or even x-ray diffraction (XRD), both wide and small angle, can be influenced by layers of CdSe NCs or self-assembled areas above or below the faceted crystals, which are irrelevant to the internal structure of the faceted crystals. Meanwhile, separation and purification that would simplify direct characterization is hard to perform for the small size of crystals and their softness. These are probably the reasons why conclusions that these crystals are faceted SLs were based mainly on their optical color and the presence of organized self-assemblies observed by TEM in their vicinity.

However, using only simple observations in the optical microscope, we can say that these faceted crystals probably are not related to SLs. The first evidence comes from their examination between the crossed polarizers (Fig. 1b). Cubic structure, produced by close-packed randomly oriented NCs, has been reported in all studies of CdSe 3-D SLs [8]. Meanwhile, all faceted crystals presented in Fig. 1 exhibit bright polarization colors that may correspond to any crystal symmetry except for cubic. Well-pronounced uniform polarization colors that go to extinction every 90° imply high perfection, non-cubic crystallographic lattice. In contrast, TEM images of SLs in [12,13] show the same simple cubic *fcc* structures with often irregularly shaped, randomly oriented NCs that are not assembled in perfectly straight arrays. The next unexpected result comes from examination by fluorescence microscopy. In all cases, independent of the photoluminescence (PL) color of the initial NCs, the faceted crystals are dark (Fig. 1c). The absence of luminescence on the surface, as well as in the bulk of the crystals, was confirmed additionally by our laser studies [17]. More complete characterization was made when, after some experience, we could produce faceted crystals in a much wider range of sizes, which made them available for direct measurements by TEM and X-ray diffraction. To obtain crystals for TEM analysis, several grids were placed on a glass slide and covered with a drop of a

NC solution, which typically produced many faceted crystals as observed by optical microscopy. After the drop dried, the grids were collected, and despite the fact that most crystals were still too thick, smaller and thinner crystals transparent for the TEM beam could also be found. One such crystal with definite hexagonal faceting that can be seen at any magnification is shown in Fig. 2a. The wide-angle e-diffraction obtained from this area shows the pattern of a bulk single crystal, and a higher magnification TEM image does not reveal any organized assemblies of NCs within or around the crystal (Fig. 2b). Similar results were obtained with many other small crystals precipitated on the grids. Much larger crystals, with the sizes approaching 1 mm, could be found in some solutions on the bottom of the glass vials. Careful removal of the solution, followed by washing the crystals with methanol, allowed for their complete separation from the NC powder. Examples of such isolated crystals are shown in the Fig. 2c and d. Both EDS analysis of a crystal on a TEM grid and of a group of crystals placed in a narrow glass capillary for X-ray diffraction, unambiguously showed that the investigated faceted crystals are in fact α -phase red monoclinic Se. This identification of the crystals was also confirmed by synchrotron analysis (not shown here), and by our additional experiments, such as comparison of melting points of commercial Se particles placed on a microscope slide next to the faceted crystals. Despite the very low solubility of Se, we could manage to obtain the same platelets from solutions of pure Se in toluene. It took several month to dissolve a sufficient amount of Se in toluene and then to produce the crystals by slow evaporation (Fig. 1e). α -phase Se is known for its crystallization from solutions in the shape of hexagonal platelets with the color of crystals varying from yellow to deep-red depending on their thickness and impurities [18]. The mechanism of Se formation that obviously relates to the stability of NCs is not completely clear. Without trying to make it a special subject of this paper, we nevertheless can say that, most likely, Se forms as a result of some transformation in the NCs. In the experiments performed with only Se precursor injected into the TOPO mixture, no precipitation occurred upon addition of methanol in the final step of the syntheses, and no Se peaks were ever observed in XRD patterns of fresh powders, even those synthesized with an excess of Se. This suggests that excessive Se may be initially a part of the NC core structure, or may be attached to the surface as a complex with TBP (TOP). Since formation of well defined Se crystals was not observed in the samples stored in a glove box, it may be slowly released into the solutions as a result of oxidation process. It obviously can be accumulated in solutions in the metastable state in an amount largely exceeding its solubility

until fast crystallization starts producing faceted crystals. One more explanation may relate to the change of the phase diagram that can result in precipitation of Se, as it was described in [19] for the case of ZnSe bulk crystals.

It is hard to say how the precipitation of Se changes the optical properties of the NC solutions. No change in the absorption spectra has been noticed, although this fact can be explained simply by the low amount of Se precipitation compared to CdSe. The change of PL spectra is difficult to interpret, because a possible effect due to the Se precipitation is screened by the noticeable red shift of the PL peak position with the CdSe NC concentration increasing during the evaporation [20]. We also did not see any correlation between the rate of Se precipitation and quality of the initial NCs.

Meanwhile, in NCs samples of high quality as indicated by their absorption and PL spectra, we frequently observed by TEM perfectly organized self-assemblies extended in many cases for hundreds of nanometers. There is no need to describe these structures, which were thoroughly investigated in previous works [8]. However, examining drops produced from such samples on a microscope slide, we could find areas with very distinctive surfaces consisting of periodically repeated geometrical figures similar to those shown in Fig. 3a. Amorphous structures cannot form such geometrical patterns on surfaces due to the lack of periodicity. That is why surfaces of amorphous (glassy) CdSe NC solid layers are typically flat or consist of randomly shaped figures (insert in Fig. 3a). Geometrical figures attributed only to organized periodic structures are common for the surfaces of bulk crystals and epitaxial single crystal layers [21]. They reflect the structure of growth hillocks, steps, dislocations or other defects in crystallographic lattice (Fig. 3b). Considering a direct correlation between the appearance of these geometrical surfaces and the observation of massive amounts of SL in TEM, we assumed that such surfaces with geometrical patterns belong to 3-D, microscopic scale, crystallographic assemblies of NCs. To promote better conditions for their formation, we replaced simple crystallization in a drop by a slightly improved growth technique. In this case, a quartz slide was placed on the bottom of a Petri dish that subsequently was filled by diluted NC solution in toluene. Dilution, accompanied by vigorous stirring prior to the growth, was made in order to break the random clusters that are always present in concentrated solutions. Several TEM grids were placed on a slide; then the Petri dish was covered and left for slow evaporation of the solvent. Parallel runs were made in air and a glove box. Examination of the slides in an optical

microscope after the solvent evaporation, revealed layers consisting of separate randomly oriented islands without faceting, but with well-pronounced parallel surface features intersecting at 60° , 120° or 90° angles (Fig. 3a). In air-free experiments, homogeneous areas with periodic parallel features could reach sizes close to 1 mm (Fig. 3c). Careful records were made about the surface structure in the location of each grid, and then the grids were separated from the slide for further analysis. TEM images from the grids taken from the layers without any visible surface structure showed mainly amorphous packing of NCs. Meanwhile, all grids removed from the areas with the geometrical features on the surface, showed the predominant existence of thick layers of NCs organized into extended 3-D SLs in all areas available for TEM analysis (Fig. 3d and e). At low TEM magnification, some individual SLs can even seem to be faceted (Fig. 3d). However, at higher magnification these quasi-facets loose their sharpness revealing a gradual slope instead of an abrupt crystal edge. Small-angle electron diffraction patterns (insert of Fig. 3e) obtained from different parts of SLs are consistent with a cubic structure. However, the orientation of individual NCs within a SL is mostly random. Some degree of the preferred orientation indicated by the discrete structure of the wide-angle electron diffraction rings shown in the insert of Fig. 3c is typical only for SLs formed from bigger NCs. At smaller size, the orientation of the individual units is fully isotropic (insert of Fig. 3f), which means that they represent pure molecular crystals formed only by the weak Van der Waals interaction between the building units. The weak interaction between NCs in SLs is fully consistent with their properties, which are typical for molecular-type crystals. They are soft and easily dissolved producing solutions with exactly the same optical characteristics as the initial NCs. They have bright PL colors, and as cubic structures, they are not seen between crossed polarizers. The lack of precise alignment between the individual units may prevent a perfect faceting of SLs. However, the biggest obstacle still comes from size and shape distribution combined with a thick and most likely not uniform surfactant layer. Estimations made from about 40 SL images showed that the spacing between particles stays relatively constant within a continuous individual SL, varying, however, substantially in different SLs. The range of SL spacing calculated for the grids placed in different locations of the same solid layer obtained from 3.3 nm NCs was from 5.42 ± 0.08 nm to 6.36 ± 0.09 nm, with the respective surface-to-surface distance between the particles from 2.95 nm to 4.04 nm. Such large variations, which are most likely responsible for

the formation of poly-domain structures, should also lead to fluctuation of the optical properties within a solid layer.

Figure 4 shows first results of optical characterization made separately on SLs and amorphous solid layers of CdSe NCs. Different structures of the solid layer deposited on a quartz slide were easily identified in the microscope allowing focusing a laser beam in precise locations of a NCs layer. Photo (a) shows a luminescence image of an area that includes amorphous layers indicated by points 1-3 with isotropic surface structure, some mixed area (points 4-7) with a collection of differently oriented small SLs, most likely mixed with some amorphous parts, and an extended SL (points 8-12) with a highly organized surface structure. Figs. 4b and c show absorption and PL spectra of the initial solution of NCs in toluene, together with the absorption of the solid layer. The absorption of the solution and solid layer fully coincide, while PL spectra of the solid exhibit a red shift with the peak position fluctuating in different locations of the layer (Fig. 4d). The red shift was described previously in [8], and attributed to electronic energy transfer between different size NCs, also known as long-range resonance transfer (LRRT) [22]. In LRRT, the PL of smaller dots is partially reabsorbed by the larger ones, producing thus a decrease in the PL quantum yield (QY) of the smaller NCs and an increase of the QY for the larger NCs. Since the efficiency of the LRRT process strongly depends on the distance between NCs, we would expect that the fluctuation of the peak position results from variations in the local packing of the amorphous layers. The same phenomenon can explain the fluctuating structure of the spectra taken in the mixed area (Fig. 4e), where LRRT can be even more influenced by the inhomogeneity produced by SLs with different spacing and amorphous layers. This interpretation is supported by the last set of spectra obtained from different points of the SL (Fig. 4f). All spectra measured in these and many other locations show precisely the same shape and peak position due to the constancy of the lattice parameters within the individual SL. However, an unexpected result here is the double structure of the spectra. Varying only slightly in intensity, they represent an obvious superposition of two spectra (shown by dashed lines) with constant ratio of the QYs across the SL. Such structure can hardly be produced by the presence of random amorphous particles in the measured locations, since in this case we would expect variation in the position and intensity of the peak. More likely it is connected with the partial efficiency of the LRRT, when only a fraction of the energy is transferred from smaller NCs to the larger ones [8]. This suggestion would be in agreement with the variations in the ratio of QYs in the double-

structured spectra of the mixed areas and its constancy in the SL. However, it still does not explain a curious fact that the positions of two individual peaks in the SL spectra correspond to the shortest (565 nm) and longest (580 nm) wavelengths measured over the entire solid layer on the slide. All these phenomena require further investigation using broader varieties of NCs types and sizes. In this respect, the fact that optical measurements can be made selectively in the structures with different packing opens new opportunities for studying the phenomena of energy transfer in NC solids.

In summary, faceted crystals that have been identified in previous works as SLs grown from CdSe NCs were analyzed. The results of optical and electron microscopy combined with x-ray diffraction presented here show that these faceted shapes are instead single crystals of red α -phase Se that form most likely as a result of oxidation of the NCs. Microscopic-scale SLs, with the size up to 1 mm, were obtained within epitaxial solid layers precipitated on quartz slides from CdSe NC solutions. Selective measurements made in SLs and in amorphous areas showed that PL spectra remain constant over an individual SL, but vary in amorphous and mixed areas. These results are explained by a change in the efficiency of energy transfer with variations of the distance between NCs, which remains constant within an individual SL and vary in amorphous and mixed areas. However, the double-peak structure of the PL spectra of SLs is not fully understood and should be investigated further in SLs produced by more advanced growth techniques and larger varieties of NCs.

Experimental

CdSe NCs were synthesized using standard air-free techniques [14 -16]. Precursor prepared from 0.37 g of dimethylcadmium $\text{Cd}(\text{CH}_3)_2$ (STREM Chemicals) and 0.148 g of Se powder (Aldrich) co-dissolved in 9.481 g of tri-n-butylphosphine TBP (STREM), was stored in a refrigerator prior to the experiment. Technical TOPO (Alfa Aesar) was evacuated at 110° C and heated under Ar to 360° C. 3 ml of the precursor mixture was quickly injected into the TOPO solution, and the reaction was allowed to continue until a desired size of NCs, monitored by measurements of UV-visible absorption, was reached. The amount of TOPO was from 6 to 8 g, and the time of the reaction varied from 5 to 50 min depending on the size of the final crystals. In some experiments, the mixture of TOPO (99% purity, Aldrich) and tetradecylphosphonic acid (TDPA, Alfa Aesar) in the Mol ratio 92:8 was used instead of technical TOPO, as well as n-trioctylphosphine (TOP) was used instead of TBP. Initial Cd precursors could also vary leaving the composition of Se precursor and the Mol ratio Cd:Se constant in different runs. These alternative routes [16], however, did not affect the results described in this paper. Reactions were terminated by removing heat. Methanol was added at approximately 50° to precipitate NCs that were further separated by centrifuging, additionally washed by methanol at least 3 times and dried under Ar flow. Absorption of the final NCs in toluene solutions was measured using a Shimadzu UV-visible spectrophotometer. PL spectra were obtained using a collimated 488nm Ar⁺ laser combined with a confocal microscope. The laser was focused to a spot size of 10 microns, allowing for the acquisition of PL spectra from specific points on a microscope slide. Optical observations were made by Olympus polarization and fluorescence microscopes with maximum magnification of 2500. TEM images were obtained at UC Berkeley and at Livermore Lab using a TEM Tecnai-12 with accelerating voltages

100kV and a HRTEM Philips CM300FEG, 300 kV. Lattice spacing was calculated by 2-D fast Fourier transform on the TEM images in MATLAB. X-ray diffraction was taken by the CPS 120 INEL curved, position sensitive detector system utilizing Cu K α radiation.

Acknowledgment. The authors thank J.Harper for performing the HRTEM, and S.Fakra and M.Marcus for synchrotron measurements. This work was performed under the auspices of the U.S. Dept. of Energy at the University of California/Lawrence Livermore National Laboratory under contract no. W-7405-Eng-48.

Literature

- [1] C. B. Murray, C. R. Kagan, M. G. Bawendi, *Science* 1995, 270, 1335.
- [2] P. Alivisatos, *Science* 2001, 289, 736.
- [3] C. Collier, T. Vossmeier, and J. R. Heath, *Annu. Rev. Phys. Chem.* 1998, 49, 371.
- [4] C. Murray, S. Sun, W. Gashler, H. Doyle, T. Betley, C. Kogan, *IBM J. Res. & Dev.* 2001, 45, 47.
- [5] F. X. Redl, K. S. Cho, C. B. Murray, S. O'Brien, *Nature* 2003, 423, 968.
- [6] Z. L. Wang, S. A. Harfenist, R. L. Whetten, J. Bentley, and N. D. Evans, *J. Phys. Chem. B* 1998, 102, 3068.
- [7] S. Yamamuro, D. F. Farrell, and S. A. Maletich, *Phys. Rev. B* 2002, 65, 65.
- [8] C. B. Murray, C. R. Kagan, M. G. Bawendi, *Annu. Rev. Mater. Sci.* 2000, 30, 545.
- [9] V. I. Klimov, A. A. Mikhailovsky, Su Xu, A. Malko, J. A. Hollingsworth, C. A. Leatherdale, H.-J. Eisler, and M. G. Bawendi, *Science* 2000, 290, 314.
- [10] W. K. Burton, N. Cabrera, F. C. Frank, *Philos. Trans. R. Soc. London A* 1951, 243, 299.
- [11] R. L. Whetten, J. T. Khoury, M. M. Alvarez, S. Murthy, I. Vezmar, Z. L. Wang, P. W. Stephens, C. L. Cleveland, W. D. Luedtke, and U. Landman, *Adv. Mater.* 1996, 8, 428
- [12] D. Talapin, E. Shevchenko, A. Kornowski, N. Gaponic, M. Haase, A. Rogach, H. Weller, *Adv. Mater.* 2001, 13, No. 24, 1868.
- [13] A. L. Rogach, D. V. Talapin, E. V. Shevchenko, A. Kornowski, M. Haase, and H. Weller, *Adv. Mater.* 2002, 12, 653.
- [14] X. Peng, M. C. Schlamp, A. V. Kadavanich, A. P. Alivisatos, *J. Am. Chem. Soc.* **1997**, 119, 7019.
- [15] C. B. Murray, D. J. Norris, M. G. Bawendi, *J. Am. Chem. Soc.* 1993, 115, 8706.
- [16] L. Qu, A. Peng, and X. Peng, *Nanoletters* 2001, 1, 333.
- [17] F. R. Leon, N. Zaitseva, D. Gerion, T. Huser, D. Krol, *Proceedings of MRS Fall meeting* 2003, Symposium N (accepted for publication)

- [18] D.M.Chizhikov and V.P. Shchastlivyi, *Selenium and Selenides*, Collet's Publishers, London and Wellingborough 1968.
- [19] K.T. Chen, M.A.George, Y.Zhang, A.Burger, C.H.Su, Y.G.Sha, D.C.Gillies, and S.L.Lehoczky, *J.Cryst.Growth* 147 (1995) 292.
- [20] S.M.Liu, H.Q.Guo, Z.H.Zhag, R.Li, W.Chen, Z.A.G.Wang, *Physica E* 2000, 8, 174.
- [21] A.A. Chernov, in *Modern Crystallography*, Berlin:Springler, vol.3, 1984.
- [22] T.Forster, in *Comparative Effects of Radiation*, New York:Wiley, 1960.

Figures

Fig.1. Faceted crystals formed from CdSe NCs solutions in toluene: a) Optical photographs in transmission light. Circled are random clusters of NCs; b) Same crystals between crossed polarizers. Bright colors show non-cubic symmetry. Arrows correspond to the positions of light extinction. Circled NC clusters are dark, that relates to isotropic structure; c) Images taken in luminescence microscope show absence of luminescence in faceted crystals compared to bright luminescence of NC background and clusters (circled). d) Similar faceted crystals obtained by “controlled oversaturation technique” [12, 13] and e) from solution of pure commercial Se in toluene. Crystal dimensions vary from 20 μm to 800 μm .

Fig.2. a) Low magnification TEM image of a hexagonal platelet crystal with an electron diffraction pattern (insert) of a Se single crystal. Scale bar 2 μm ; b) Higher magnification TEM image of the crystal corner does not show any organized structure in the arrangement of 3.5 nm NCs near or on the surface of the faceted hexagon. Bar is 50 nm; c) EDS obtained from a crystal separated on a TEM grid (insert); d) Wide-angle XRD pattern of a group of separated crystals (insert) corresponds to red monoclinic α -phase Se.

Fig.3. Images of CdSe SLs. a) Optical images of geometrical surface patterns of ordered NC SLs. Insert shows surface structure of a randomly packed solid. Bar is 10 μm . The color of the images is artificially produced by reflection interference imaging; b) TEM image of an assembly of 5.2 nm NCs showing a linear defect on the border of two regions with different orientation. At larger scale, such defects can produce geometrical patterns on the surface of SLs. Bar is 20 nm. Wide-angle electron diffraction pattern with modulations in rings (insert) shows some degree of a preferred orientation of the individual NC axes; c) Optical photograph of a near 1 mm-size 3-D single SL (1) surrounded with islands of smaller SLs (2). The size of initial NCs is 3.3 nm; d) Low magnification TEM image of quasi-faceted 3-D SLs of 3.3 nm NCs. Bar is 500 nm; e) A part of a 3-D SL squared in the previous image. Small-angle electron diffraction pattern (insert) is consistent with *fcc*

structure with a lattice parameter of 5.6 nm. Bar is 50 nm; f) HRTEM image taken from the same region shows fully isotropic orientation of 3.3 nm NCs within a SL that is also confirmed by a continuous structure of wide-angle electron diffraction pattern rings (insert). Bar is 10 nm.

Fig. 4. Optical characteristics of differently packed areas of CdSe solids obtained from 3.3 nm NCs: a) Luminescence microscope image that includes randomly packed glassy solid (points 1-3), collection of small partially organized and glassy areas (points 4-7), and extended SL with uniform surface structure (points 8-12). Bar is 500 μm . The insert shows 50x50 μm^2 area with a laser beam; b) Absorption spectra of initial solution and solid. The peak remains at the same position in all points shown in the picture a; c) PL spectra of the initial diluted solution; d) PL spectra of glassy solid in point 1-3 with fluctuating peak position; e) PL spectra of partially organized areas (points 4-7). Each spectrum shows competition of two peaks (dashed) with changing mutual intensity and fluctuating position; f) PL spectra taken from any point within the SL (points 8-12) have precisely same structure and position of two peaks with the constant ratio of QYs.

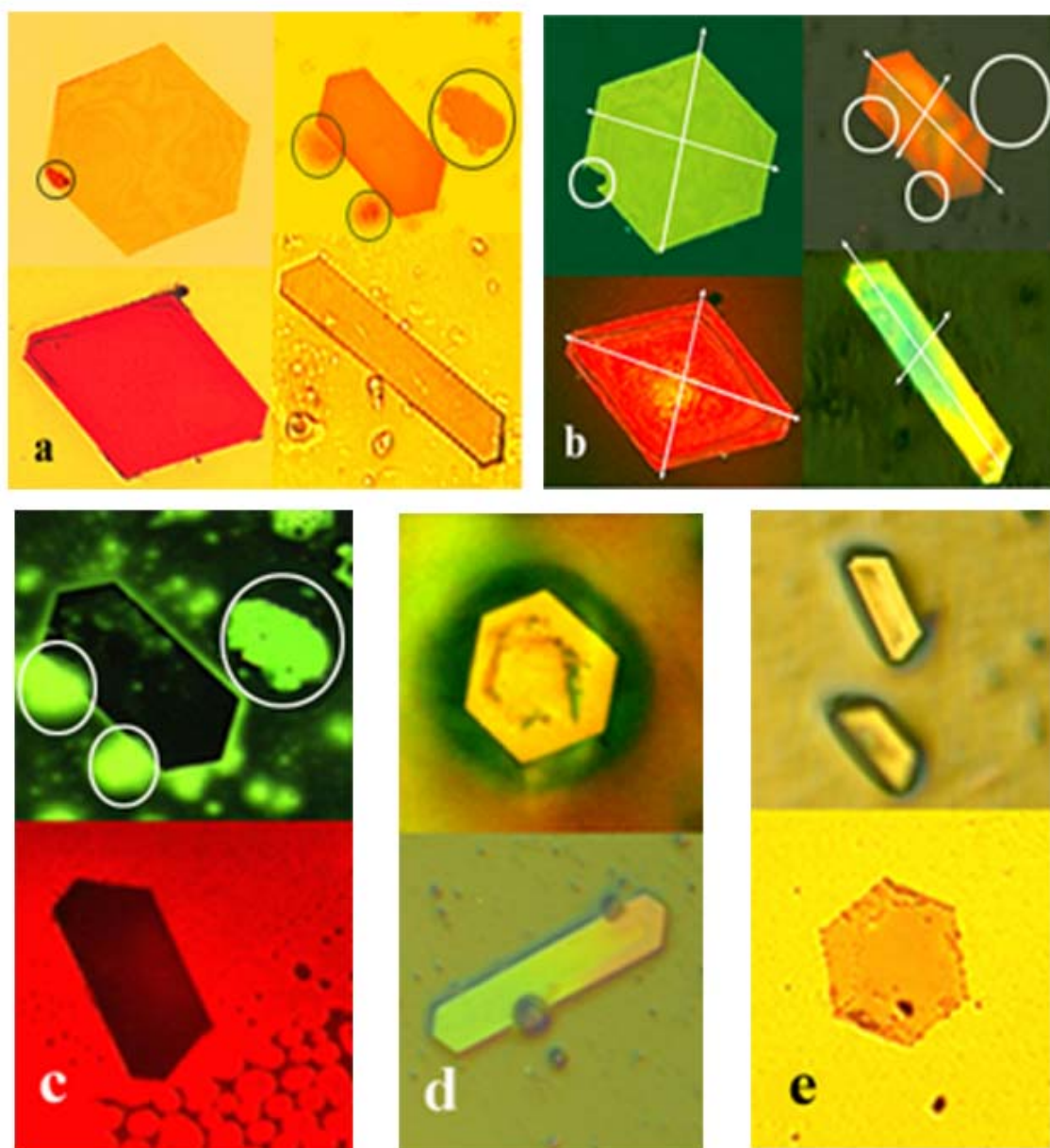
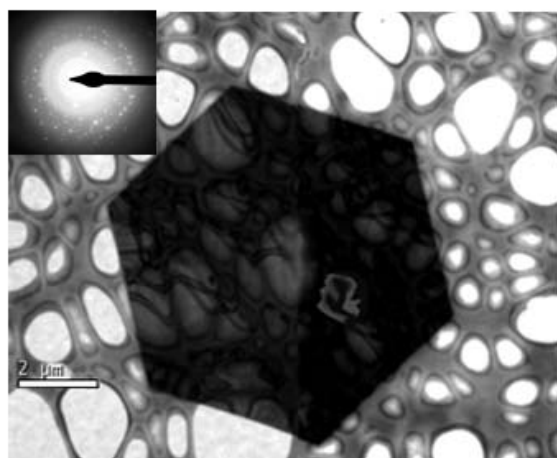
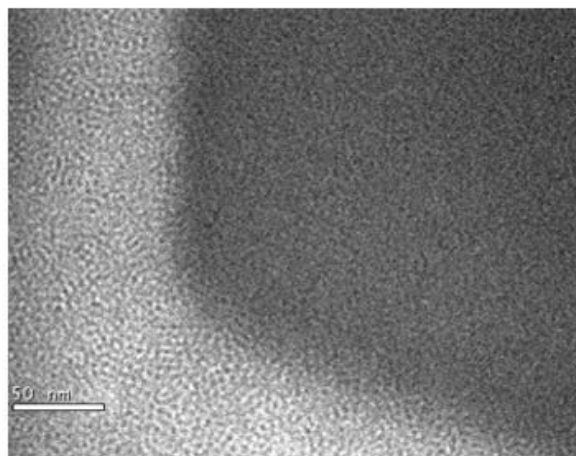


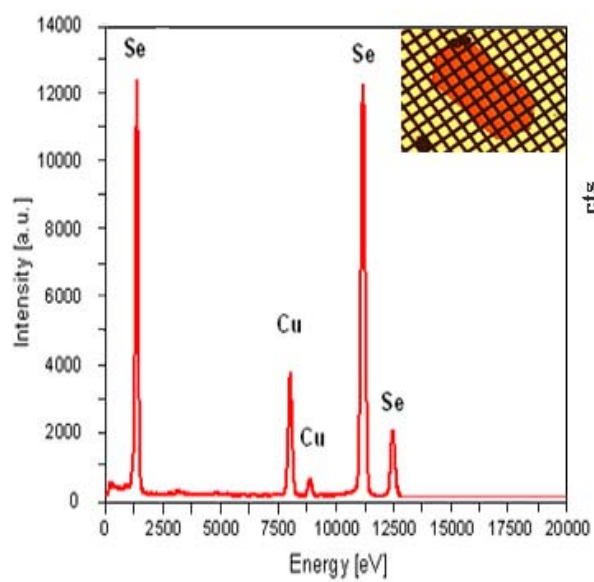
Fig. 1



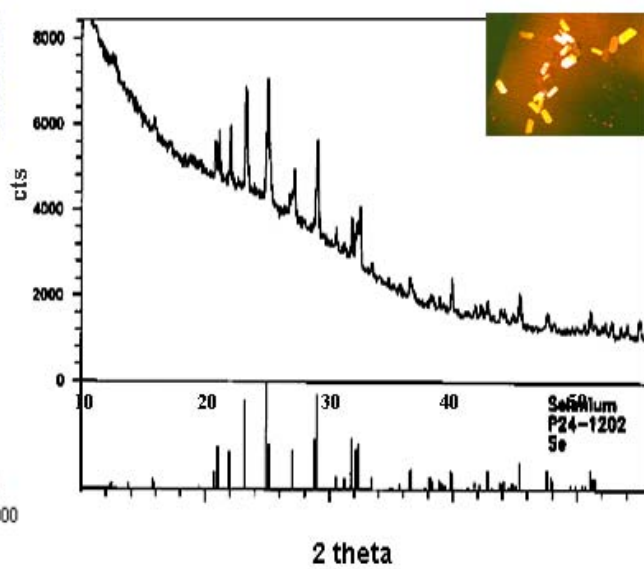
a



b



c



d

Fig. 2

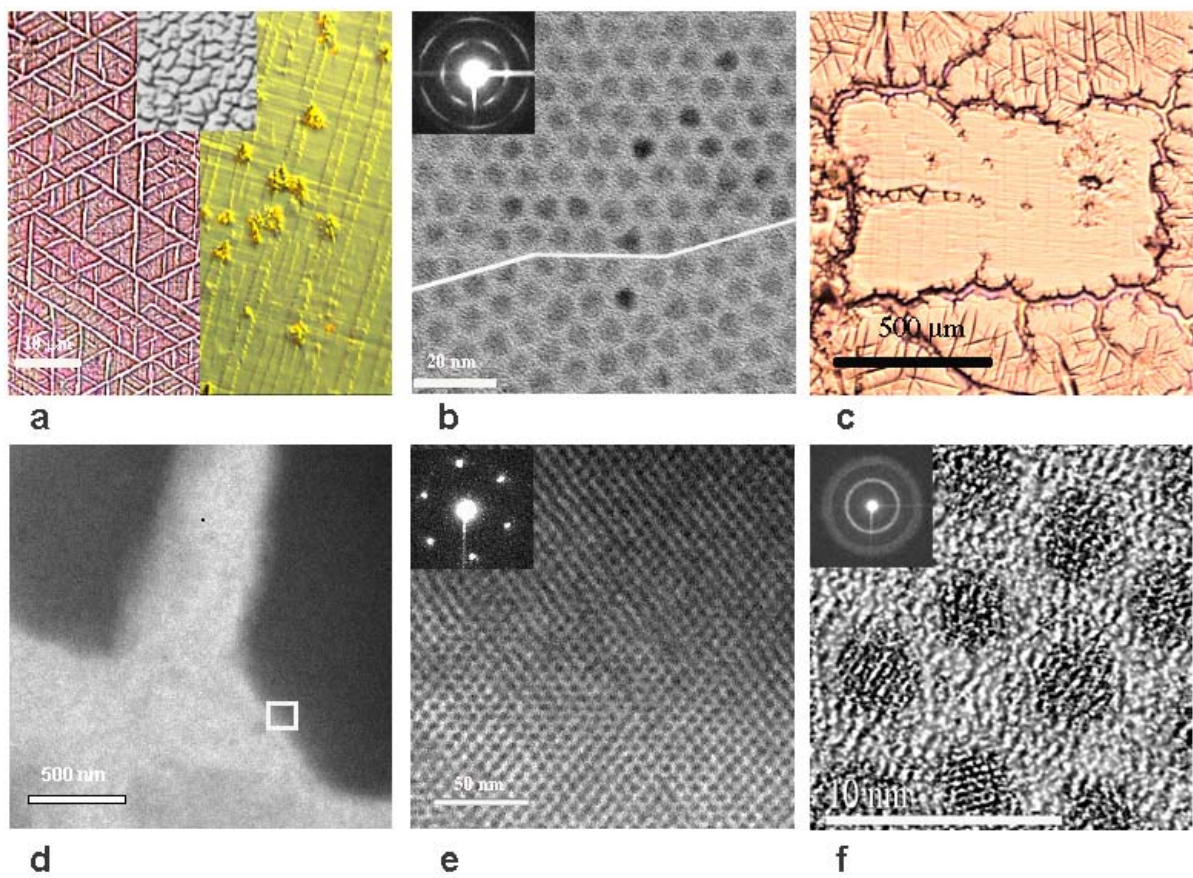


Fig.3

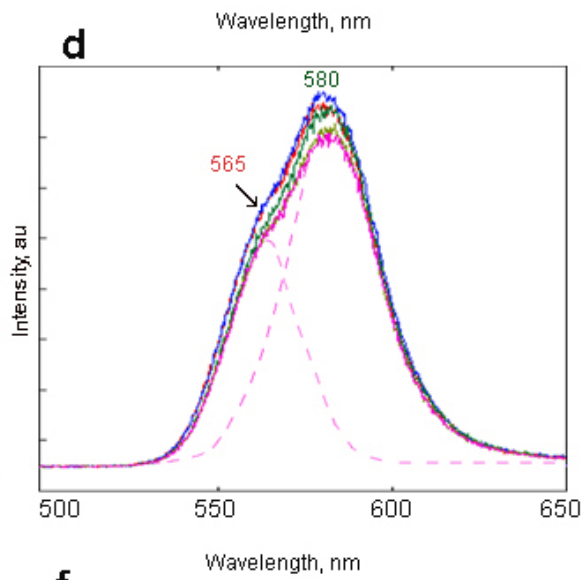
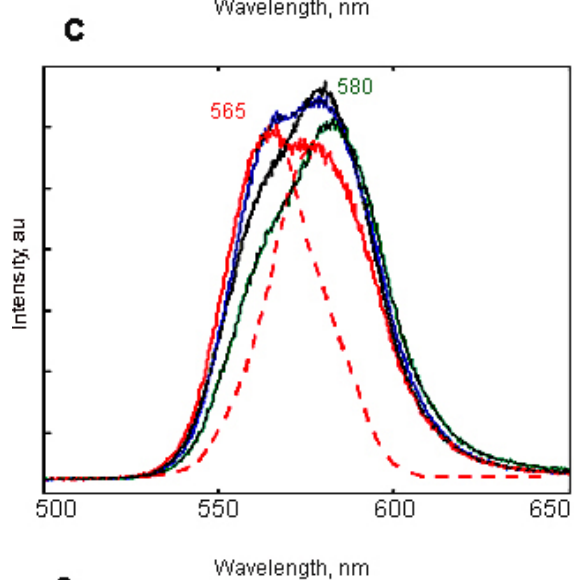
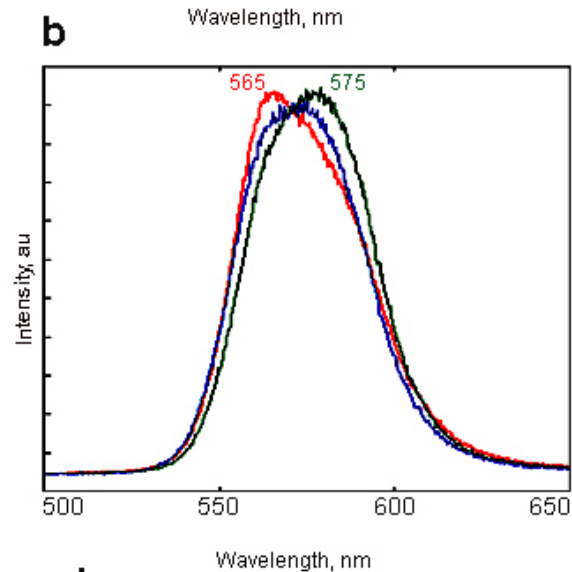
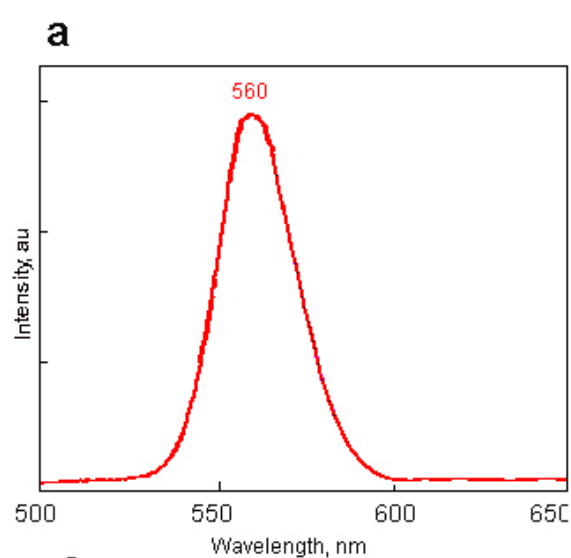
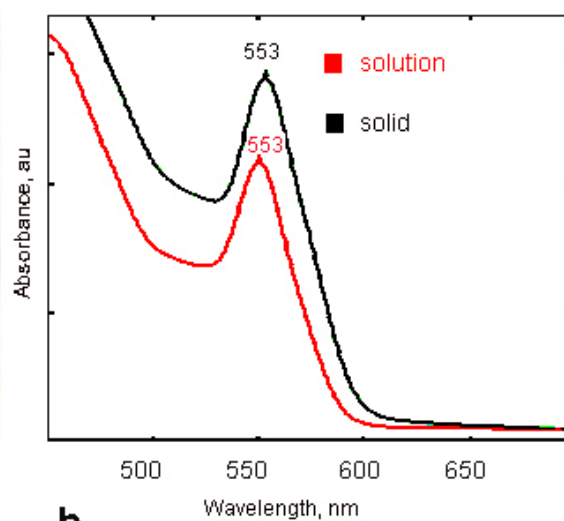
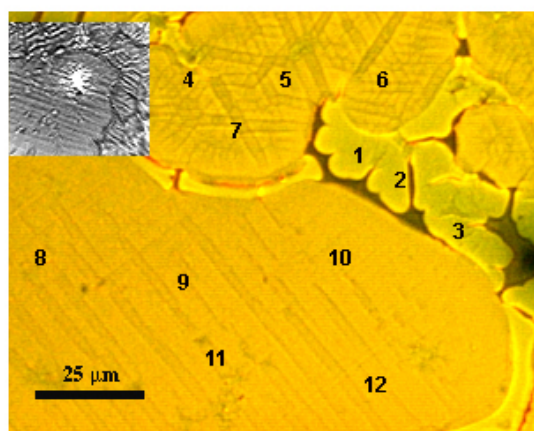


Fig. 4

